USGS
science for a changing world

Techniques of Water-Resources Investigations
of the United States Geological Survey

CHAPTER D1

APPLICATION OF SURFACE GEOPHYSICS
TO GROUND-WATER INVESTIGATIONS

By A. A. R. Zohdy, G. P. Eaton,
and D. R. Mabey

BOOK 2
COLLECTION OF ENVIRONMENTAL DATA

Seismology

By G. P. Eaton

Applied seismology has, as its basis, the timing of artificially-generated pulses of elastic energy propagated through the ground and picked up by electromechanical transducers operating as detectors. These detectors, or geophones as they are more commonly called, respond to the motion of the ground, and their response, transformed into electric signals, is amplified and recorded on magnetic tape or film on which timing lines are also placed. The geophysicist is interested in two parameters which affect the elapsed time of transmission of this pulse— the propagation velocity (or velocities) and the geometry of the propagation path. The determination of these parameters is a complex task, both in practice and in theory. Energy generated at the source travels in several types of waves simultaneously, and each wave has a different transmission velocity. Furthermore, each of these waves may travel to the geophones by more than one path. For example, the first energy to arrive at a geophone near the source may arrive via the direct wave; that is, the energy travels parallel to the surface in the layer in (or on) which the source and receiver are located. Another geophone, located farther away, may record the arrival of a refracted wave first. When such a wave impinges on a sub-horizontal discontinuity where there is an abrupt change in elastic properties, reflection or refraction of the wave will lead to the generation of additional waves. Thus a compressional wave can give rise to both a reflected and refracted compressional wave and a shear wave. Lastly, energy travelling into the ground may return to the surface via reflections or refractions from several different interfaces of varying depth. The geophysicist must be able to recognize and sort out from the complex wave train arriving at the geophones those impulses in which he is interested and must translate their times of transmission into geological information.

Elastic wave energy can be imparted to the ground in a variety of ways. The most commonly used method is that of firing a charge of explosives with high detonation velocity in a tamped hole. Such charges may be fired on the surface or a short distance above it. The amount of charge used depends on the length of the propagation path and the attenuation characteristics of the earth materials along the path. Although crude rules-of-thumb for estimating the explosives requirements for a given shot have been formulated, there is enough variation in attenuation characteristics from area to area that the requirements at a given locale are best determined by trial and error; so also are the depth-of-shot requirements. In some areas, and for some kinds of records, the seismologist may require a drilled or augered hole below the water table. In others, he may be satisfied to place the charge in a shallow, hand-dug hole and tamp it with a shovelful of soil. In still others, he may wish to excavate a hole of intermediate depth, say 3–5 m (10–15 feet), with a backhoe and then refill the hole with earth. In general, the deeper the target, the larger the charge, and the larger the charge, the greater depth of implantation. The bulk of the explosive energy should be consumed in producing elastic waves. If much energy is spent in the process of venting, the shot probably will not be efficient and the desired results will not be obtained. For very shallow work (20 m (65 feet) or less) adequate energy sometimes can be generated by a hammer blow on a steel plate. Analogous sources of energy

in larger amounts are produced by weight dropping or by impacting the ground with a plate driven hydraulically.

Elementary Principles

The theory of elasticity on which we base our understanding of elastic wave propagation treats materials as homogeneous and isotropic. Although naturally occurring rocks, in place, do not fit either specification very well in many areas, this theory has proved to be extremely useful in understanding seismic phenomena. Actually, what are sought in seismic prospecting are the very discontinuities which make the crust inhomogeneous. These discontinuities, between bodies of unlike elastic properties, are studied and interpreted in terms of their nature, depth, location, and configuration. In most earth models they correspond to significant geological boundaries. In some settings, however, they do not, and this poses an additional problem for the interpreter.

According to the theory of elasticity, a homogeneous, isotropic, elastic solid can transmit four kinds of elastic waves. Two of these, the compressional (or longitudinal) wave and the shear (or transverse) wave, are body waves. They are transmitted through the interior of the solid. In the passage of a compressional wave, particle motion in the medium is parallel to the direction of propagation, like that of a sound wave in air. The particle motion created by a shear wave is perpendicular to the direction of propagation. The other two waves, known as Rayleigh waves and Love waves, are confined to a region near the free surface of the medium; their amplitudes decrease with depth in the medium. They are also referred to as surface waves. The particle motion created by these surface waves is complex; Love waves, for example, require a surface layer with elastic constants different from those of the rest of the solid. Very little use has been made of the propagation of shear waves or surface waves in

hydrogeology. However, suggestions have been made as to how they might be used to advantage in ground-water studies (Eaton and Watkins, 1970). Nothing more will be said of shear or surface waves in the paragraphs that follow—all reference to elastic wave propagation from this point on is concerned with compressional waves. These waves have the highest velocity of the four types discussed and, therefore, the shortest traveltime for a given propagation path.

Elastic energy moves outward from a point source in a series of waves with curved fronts. For illustration, the path which the energy follows from source to geophone is most easily defined by a ray, a line drawn normal, or nearly normal, to the wavefront, depending on whether or not the medium is isotropic. The ray-paths which seismic energy follows are constructed by the method of geometrical optics.

The paths of four rays emanating from a point source of energy at the surface are shown in figure 54. The model is that of a horizontally layered earth, where the seismic wave velocity, V_1, of the upper medium, is less than the velocity of the underlying medium, V_2. These four rays are:

1. The direct ray, which travels a horizontal path from source to receiver.
2. The totally reflected ray, which is generated when a ray strikes the boundary between the two media at an angle of incidence i_1 greater than the critical angle i_c, and all of the energy is reflected back toward the surface.
3. A ray striking the boundary at precisely the critical angle of incidence i_c, part of the energy being reflected back toward the surface and part refracted, the latter travelling parallel to the interface with velocity V_2.
4. A ray striking the interface at an angle of incidence i'_1, less than the critical angle, part of the energy being reflected upward and part being refracted in the lower medium away from the normal to the surface, at angle r. The magnitude of r is a function of the ratio
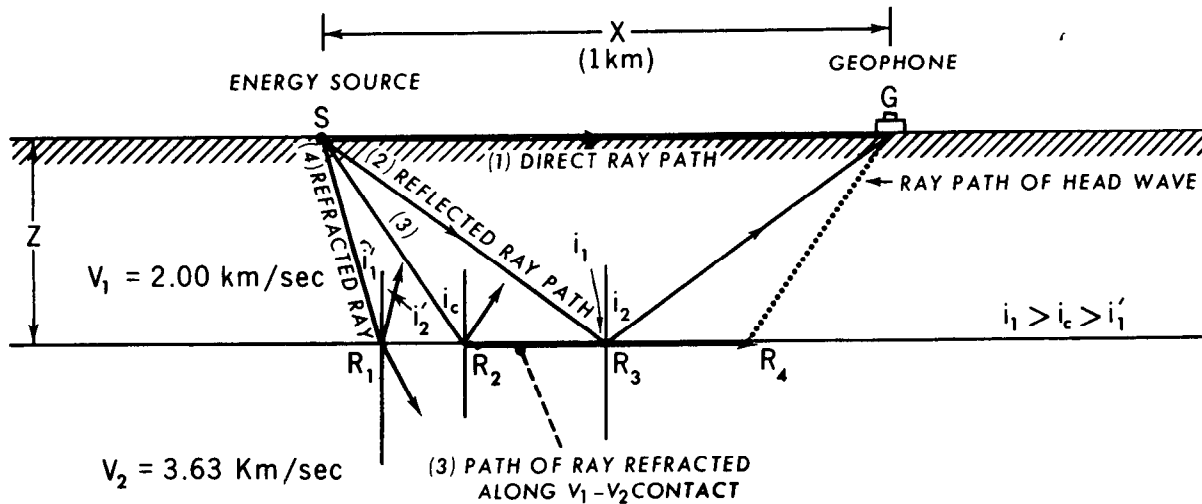
Figure 54.—Schematic ray-path diagram for seismic energy generated at source S and picked up at geophone G. Traveltimes for the various rays are as follows: t_1 = 0.500 sec, t_2 = 0.630 sec, and t_3 = 0.588 sec.

of the two velocities and the angle of incidence (see eq. 1). Division of the incident energy between reflected and refracted waves depends on the angle of incidence and the contrast in velocities and densities of the two media.

As the pulse of energy travelling ray-path 3 moves along the interface between the two media at velocity V_2, it generates a small disturbance or pulse in the lowermost part of the upper medium. Energy from this disturbance eventually reaches the surface of the ground where it is picked up by the geophone.

The angular relationships among the various parts of the ray-paths just described are as follows:

For ray-path 2,

$$i_1 = i_2 . \tag{1}$$

For the reflected branch of ray-path 4, $i_1' = i_2'$, and for the refracted branch

$$\frac{\sin i_1'}{\sin r} = \frac{V_1}{V_2} \quad \text{(Snell's Law).} \tag{2}$$

At the critical angle of incidence, the angle of refraction r is 90° and sin r = 1. Thus, the critical angle can be defined in terms of the two velocities as

$$i_o = \arcsin\left(\frac{V_1}{V_2}\right). \tag{3}$$

These simple equations, plus that expressing the relationship between velocity, distance, and time, constitute the basis for the interpretation of seismic data.

As an example, consider the reflected ray-path $\overline{SR_3G}$. The relationship between the velocity, V_1, the length of the propagation path, $\overline{SR_3G}$, and the transmission time, t is:

$$V_1 = \frac{\overline{SR_3} + \overline{R_3 G}}{t}. \tag{4}$$

Now according to equation 1, $i_1 = i_2$; thus we can rewrite equation 4 as

$$V_1 = \frac{2\,\overline{RS_3}}{t}. \tag{5}$$

Because

$$\overline{SR_3} = \sqrt{(X/2)^2 + Z^2} ,$$

then

$$V_1 = \frac{2\sqrt{(X/2)^2 + Z^2}}{t}.$$

Rearranging terms, and solving for Z:

$$Z = \tfrac{1}{2}\sqrt{V_1^2 t^2 - X^2} . \tag{6}$$

The distance X in this equation is predetermined by the placement of the geophone, and the transmission time t is read from the seismogram. Thus, in equation 6 if the velocity V_1, of the upper medium is known from independent measurement, we can calculate the depth to the interface, Z.

Reflection Versus Refraction Shooting

Determination of depth by the means just described is referred to as a seismic reflection measurement. The reflection method is one of two general types of seismic measurements in common use, the other being the refraction method.

The refraction method is illustrated schematically by ray-path 3 in figure 54. The propagation path of ray 3 consists of three branches, $\overline{SR_2}$, $\overline{R_2R_4}$, and $\overline{R_4G}$, but we have not yet indicated why there should be a branch like $\overline{R_4G}$. It was mentioned earlier that energy from the disturbance travelling along path $\overline{R_2R_4}$ eventually reaches the surface. The head wave, which is the name given to the wave carrying energy upward from the disturbance at the interface, is a physical representation of Huygens' principle, which states that each point on an advancing wave front in an ideal elastic body is a source of secondary spherical waves. The wave front of these new waves at a later instant of time is defined by a surface tangent to the newly-generated spherical waves. This is illustrated in figure 55, where a, b, and c represent successive crests of a disturbance moving parallel to the interface with velocity V_2. They are, according to Huygens' principle, sources of secondary waves which will move upward in the disturbed upper medium with velocity V_1. The arcs in figure 55 represent a succession of spherical waves emanating from each of these points and the thin lines tangent to them are the wave fronts normal to which the rays travel. As a disturbance with velocity V_2 travels parallel to the interface from a to c, energy radiating upward from it travels from a to d at velocity V_1. These two paths, $\overline{ac}$ and $\overline{ad}$, define the angle ω. Thus,

$$\sin \omega = \frac{\overline{ad}}{\overline{ac}} = \frac{V_1 t}{V_2 t} = \frac{V_1}{V_2}. \quad (7)$$

A comparison of equation 7 with equation 3 indicates that the the angle ω is the same
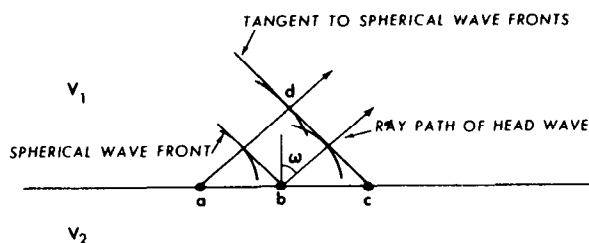

Figure 55.—Huygens' construction for a head wave generated at the V_1-V_2 interface.

as the critical angle i_c. The significance of this in figure 54 is that the right hand branch of ray-path 3 or $\overline{R_4G}$ is a mirror image of the left-hand or incident branch $\overline{SR_2}$. It follows that the relationship between the velocities V_1 and V_2, the length of the propagation path $\overline{SR_2R_4G}$, and the transmission time t can be written

$$t = \frac{\overline{2SR_2}}{V_1} + \frac{\overline{R_2R_4}}{V_2}. \quad (8)$$

The geometry of figure 54 allows us to make the following substitutions:

$$\overline{SR_2} = Z/\cos i_c \quad (9)$$

and

$$\overline{R_2R_4} = X - 2Z \tan i_c. \quad (10)$$

Substituting these expressions and that of equation 3 in equation 8 leads to

$$t = \frac{X}{V_2} + \frac{2Z \cos i_c}{V_1}. \quad (11)$$

After rearranging terms, and substituting an expression containing V_1 and V_2 for $\cos i_c$:

$$Z = \frac{V_1 V_2}{2\sqrt{V_2^2 - V_1^2}} \left(t - X/V_2 \right). \quad (12)$$

As before, the distance X is predetermined by the placement of the geophone and the transmission time t is read from the seismogram. Substitutions of these values, plus those for V_1 and V_2, in equation 12 leads to a value for the depth Z to the interface.

In making calculations of depth from reflection measurements, the velocity values

used must be determined by independent means. In contrast, refraction measurements yield values for the velocities of the formations directly, provided certain conditions are realized. Although a discussion of these conditions is beyond the scope of the manual, it may be instructive to show how the values for velocities V_1 and V_2 are a product of the refraction measurement itself.

Figure 56 shows a model of a two-layered, horizontally-stratified Earth. The compressional wave velocities of each of the layers is indicated at the right. On the surface are ten geophones recording direct and refracted wave energy from a source at the left. Directly above the model is a time-distance plot. The abscissa of this plot is horizontal distance, measured from the shot point, and the ordinate is time elapsed since the shot instant. The measured elpased time of the first arrival of energy recorded by each geophone is plotted as a point directly above the geophone. Straight lines drawn through these points constitute branches of a traveltime curve. The slope of each branch is the reciprocal of the velocity of the layer it represents. This is most readily understood from the following argument:

At distances less than X_c, the "critical distance," at which the two branches of the traveltime curve intersect, the first arrival of energy is via the direct wave. At distances greater than X_c, the first arrival is via the refracted wave. The refracted wave travels a longer path than the direct wave, but at distances beyond X_c the fraction of its total path occurring along the high velocity bed is sufficiently great to compensate for the effect of this extra distance of travel. The traveltimes indicated on the first branch of the plot (to the left of X_c) are the result of direct wave arrivals, and as such are given by the equation for direct traveltime:

$$t = X/V_1 \qquad (13)$$

Differentiating this equation with respect to X gives

$$\frac{dt}{dX} = \frac{1}{V_1}. \qquad (14)$$

From this it is seen that

$$V_1 = 1/(dt/dX) = 1/ \text{ (slope of first segment of plot).} \qquad (15)$$

The traveltimes indicated on the second segment of the plot correspond to first arrivals that reached the geophone via the refracted wave path. As such, they are given by equation 11,

$$t = \frac{X}{V_2} + \frac{2Z \cos i_c}{V_1}. \qquad (11)$$

Differentiating this equation with respect to X gives

$$\frac{dt}{dX} = \frac{1}{V_2}, \qquad (16)$$

since Z, i_c, and V_1 are constants,or

$$V_2 = 1/(dt/dX) = 1/(\text{slope of second segment of plot}). \qquad (17)$$

The thin lines in the model (fig. 56), both curved and straight, represent successive positions of wave fronts for those waves travelling to the surface by the fastest, or minimum-time, paths. The straight segments are those representing the head wave; curved segments represent direct and refracted waves. The dotted line separating the straight and curved parts of the wave fronts is an envelope of points for which the travel times of direct and head-wave pulses are the same. The diagram has been simplified by deleting those parts of the curved-wave front below the envelope and those parts of the plane-wave front above it. The omitted parts of each wave front exist and their ar-
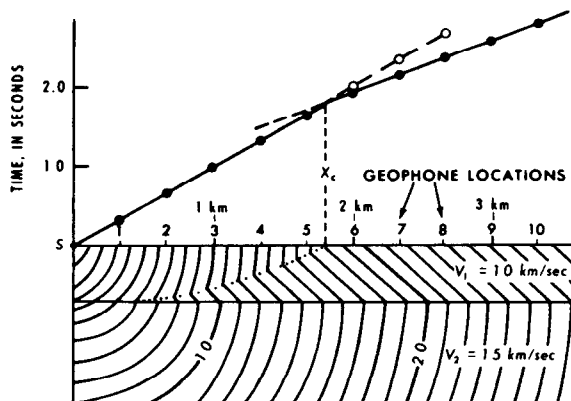

Figure 56.—Seismic wave fronts and traveltime plot for an idealized horizontally layered model. Heavy dots represent first arrivals of energy; open dots represent later arrivals. X_c represents the critical distance for the V_1-V_2 interface.

rival at the geophones constitutes a later arrival of real energy. Thus one may see on the seismogram at geophones 6, 7, and 8, an instant after the head-wave arrival, pulses that represent the arrival of a direct wave travelling with velocity V_1. These are shown in figure 56 as open circles falling on a prolongation of the V_1 traveltime branch. Such pulses are known as second arrivals. Because the amplitude of a head wave usually is much smaller than that of a direct wave, it very rarely is observed on the seismograms at distances less than the critical distance.

Comparison of the Reflection and Refraction Seismic Methods in Practice

In the preceding paragraphs, simple techniques of depth measurement by both the reflection and refraction methods have been described. How does one go about deciding which method to use in a given situation? The differences between reflection and refraction methods go far beyond the differences in ray-path geometry. These differences include geophone array (the refraction method uses much longer spreads), accuracy, resolution, depth, size and shape of the target, number of discontinuities to be mapped, vertical succession of velocity values, and cost. The great bulk of all applied seismic work done today is done by the reflection method. It offers higher accuracy and resolution, allows the mapping of a larger number of horizons, requires smaller amounts of energy, uses shorter geophone spreads (simplifying their layout and minimizing problems associated with the communication of the shot instant), and is more amenable to routine field operation. In addition it does not require, as does the refraction method, that each succeeding layer have a velocity higher than that of the layer above it. In light of all these advantages, it is reasonable to inquire why the refraction method is used at all. This is an especially relevant question here, because most seismic measurements

made in hydrogeology are refraction measurements. It is in petroleum exploration that the reflection method is so extensively used.

The reasons for use of the refraction method are several. In some areas it is almost impossible to obtain good reflection records. A typical example is an area of thick alluvial or glacial fill. In this setting optimum reflection prospecting would require the drilling of deep shot holes. Such an area lends itself admirably to the refraction method and is precisely the kind of setting in which the hydrogeologist might be interested. A downward increase in velocity can be reasonably expected in such an area and abrupt increases in velocity might be encountered both at the water table and at the base of the sediments, if they overlie consolidated bedrock. No prior knowledge of velocity is required in reconnaissance refraction measurements and the velocity information obtained in the course of the work may help in identifying the rock types involved. In reflection shooting special measurements of velocity to be made, either by greatly expanding an occasional geophone spread or by shooting at a well into which a geophone has been lowered. In the exploration of a large alluvial basin such wells may not be available to the seismologist. The reflection method works best when continuous line coverage is possible and when the line or lines can be tied to a few points of velocity control. A single reflection profile, or a series of them individually isolated and spread over many square kilometers of an alluvial basin, are not as useful as a series of isolated refraction profiles.

In areas where steeply dipping boundaries are encountered, the refraction method is better suited for exploration than the reflection method. Typical examples include a fault-bounded valley or a buried valley with steeply sloping sides.

The sophisticated equipment used in reflection work today, the relatively large size of the crews required, and the benefits derived from continuous coverage, are all difficult to justify in relation to the objectives and budget of a typical ground-water study.

The geometric subtlety of the target and the ultimate economic returns from successful exploration for petroleum do justify its use in the oil industry.

Seismic Refraction Measurements in Hydrogeology

Effect of Departures From the Simple Stratified Model

The models shown in figures 54 and 56 are highly simplified. The ground surface is perfectly plane and horizontal, the surface of the refractor with velocity V_2 is also plane, and the two surfaces are parallel. In addition, there is but one velocity discontinuity to map and there are no lateral or vertical variations of velocity within either layer. The ray-path geometry and the equations for calculating depths to the lower refractor are therefore equally simple. Such simplicity is seldom encountered in nature. The complications of real systems can be illustrated by some hypothetical models and time-distance plots.

Figure 57 shows 10 models which depart in significant ways from the simple models of figures 54 and 56. Immediately above each model is a schematic time-distance plot typical of the type that the model would generate. Ray paths are shown for models A through E, and also for model H.

The Multilayered Model
Figure 57A

Although this model is a simple extension of the horizontal two-layer model, its interpretation is fraught with practical difficulty. The thickness of each succeeding layer must be calculated individually employing a series of formulas into which one substitutes values derived for the layer immediately above it. Small errors in each step of the analysis have a multiplier effect which carries over to the calculations on each succeeding layer.

This model also requires that each layer have a velocity higher than the one above it (see fig. 57H) and that each be thick enough to produce a separate branch of the traveltime curve (see fig. 57G).

Effect of a Regular Increase of Velocity With Depth
Figure 57B

If the layers in A become vanishingly thin, they would approximate, as a group, a continuous velocity increase with depth. The result is the generation of a curved ray path in the upper medium. Such a situation is realized in thick sections of young, semiconsolidated sedimentary rocks which display increasing compaction and lithification with depth. Several velocity-depth functions have been proposed by investigators for different areas (Dobrin, 1960, p. 77; Kaufmann, 1953, table 1). The mathematics required for the calculation of depth to a lower bedrock refractor using these equations are simple enough for analytical treatment in some situations.

Effect of Dipping Layers
Figure 57C

This model illustrates the effect of a refractor that is not parallel to the surface of the ground. Geologically, this model corresponds to a series of dipping beds or to a sloping bedrock surface. In this situation the slopes of the separate branches of the traveltime curves give reciprocal values of velocity for the uppermost layer (V_1) only. In figure 57C, the slopes of the second and third branches of the traveltime curves are not reciprocals of velocities V_2 and V_3. These slopes also are not the same for the two directions of shooting (left to right, or updip, and right to left, or downdip). If a seismic profile in a geologic setting like this one were not reversed; that is, if it were not shot first from one end of the geophone spread and then from the other, there would be no way of recognizing the dip nor the erroneous values for V_2 and V_3. By reversing the pro-
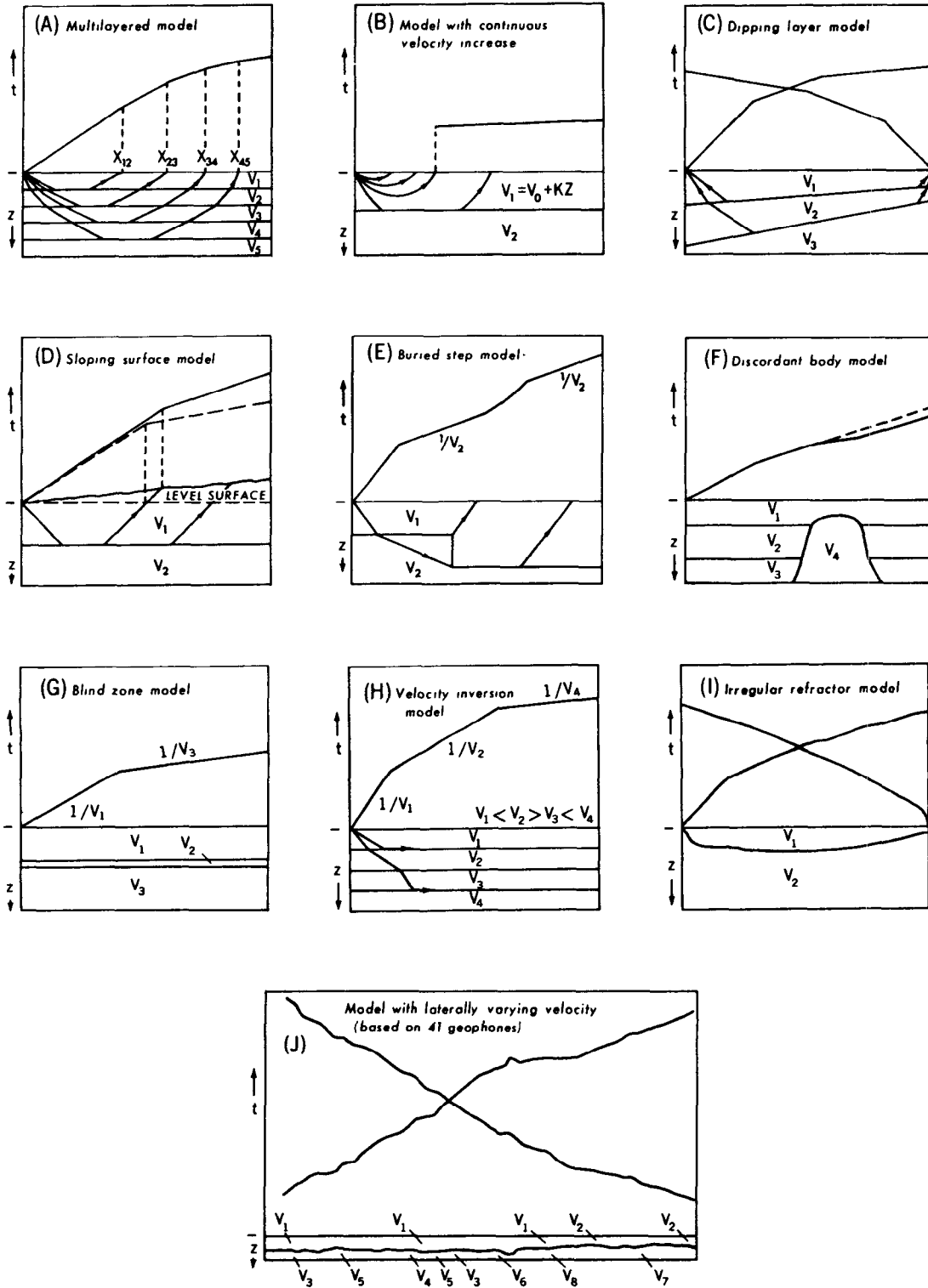
Figure 57.—Schematic traveltime curves for idealized nonhomogenous geologic models.

file, that is shooting from both ends of the geophone spread, the existence of dip is readily apparent and the dip angle can be calculated. The equations used in the calculation of dip include intermediate steps that lead to a derivation of the true values of V_2 and V_3. For a typical solution see Slotnick (1959, p. 103–118).

Effect of a Sloping Ground Surface
Figure 57D

The effect of shooting along a sloping ground surface above a horizontal refractor is somewhat analogous to that of a dipping refractor below a horizontal surface (fig. 57C). In both models the path length of rays in the upper medium varies with horizontal distance. The effect of this variation is shown in an exaggerated fashion in the time-distance plot, where the observed data are shown as solid lines, and the plot that would have been obtained if the shot and geophones had been on a horizontal surface is shown by dashed lines. Unlike the dipping refractor example, however, the slope of the ground is known before shooting and corrections can be applied to the observed arrival times. The method is discussed briefly in the section entitled "Corrections applied to seismic refraction measurements."

Effect of a Buried Steplike Refractor
Figure 57E

This model illustrates the effect of an abrupt vertical offset in a buried refractor. Geologically this could be a buried and faulted bedrock surface or a buried erosional step. Note that the two parts of the V_2 branch of the traveltime curve are parallel, but displaced from one another. This displacement is a measure of the increase in path length for rays travelling upward from the downthrown block and it can be used to calculate the vertical offset of the refractor.

Effect of a Discordant Steep-sided Body
Figure 57F

Steep-sided discordant bodies like the one illustrated may represent igneous stocks,

broad dikes, or salt diapirs intrusive into bedded sedimentary rocks. Alternatively, they might represent a buried bedrock ridge. Such a body commonly has higher velocity than the other layers and causes seismic waves travelling through it to arrive earlier than they would have otherwise. A somewhat similar time-distance plot would be obtained from figure 57E if it were shot in the opposite direction (that is, from right to left).

Effect of a Thin Refractor
Figure 57G

This illustration shows a simple three-layered model in which each layer has a velocity higher than the one above it. However, there is no traveltime branch corresponding to the layer with velocity V_2. Its absence results from the layer's thinness in relation to its depth. This condition poses a problem in interpretation if only first arrivals of energy are used in preparing the time-distance plot. What happens, in effect, is that the head wave from the thin layer is overtaken by the head wave from the higher velocity layer below it. If second arrivals are recorded, then the head wave from this layer might be seen on the seismogram. Digital seismic timers of the sort commonly used in engineering geophysics, where the arrival of a single pulse of energy is all that is recorded, would be useless in the study of a setting like this one. A layer of the V_2 type is referred to in geophysics as a blind zone. Where unrecognized, it causes error in the calculation of the depth to refractors below it. In addition, lack of knowledge of its existence may prove detrimental to the very objectives of the survey. A hydrogeologic example of this last point was illustrated by Soske (1959, fig. 6) using data from Nevada. In the area he studied, the ground consisted of consolidated bedrock with a velocity of 3.2 km/sec overlain by saturated alluvium with a velocity of approximately 2.0 km/sec. Above the water table was a zone of unsaturated alluvium with a velocity of 1.0 km/sec. The water table was at a depth of 60 meters and the bedrock at 90 meters. The

saturated zone, which was only 30 meters thick, could not be recognized from first arrivals. The presence of the saturated zone was not apparent on the time-distance plot and it appeared as though bedrock were overlain by unsaturated alluvium only.

Effect of a Velocity Inversion at Depth
Figure 57H

In this model the sequence of layer velocities from the surface downward is $V_1-V_2-V_3-V_4$, where V_3 is less than both V_2 and V_4. Layer V_3 constitutes a velocity inversion. The effect of this inversion is illustrated by the ray path in layer V_3. It is refracted downward, away from the land surface. As a result, there is no V_3 branch on the traveltime curve, for no head wave is generated by refraction below the V_2-V_3 boundary. Thus, calculations of depth to the top of layer V_4 will be in error, for the unrecognized V_3 layer will be treated as though it had the higher velocity, V_2. The result will be an overestimate of the depth to the top of layer V_4. Independent knowledge of the existence of a velocity inversion must be known from either velocity logging in a well penetrating the section, or at least suspected from resistivity measurements or knowledge of the stratigraphy, if the inversion is to be taken into account during the interpretation.

Effect of a Refractor of Irregular Configuration
Figure 57I

All the models discussed so far consist of plane refractors, either horizontal, dipping, or vertically stepped. In hydrogeologic investigations many refractors are curved and irregular. A typical example is that of a buried bedrock channel. Such a channel is illustrated schematically in figure 57I. The time-distance plot above it is irregular and lacks straight second branches that might provide a direct measure of velocity according to the methods described above. A time-distance curve of this type cannot be analyzed by customary means to extract depth

information. Much of the seismic refraction equipment manufactured for shallow or moderately deep refraction measurements includes tables, nomograms, or formulas designed to reduce depth calculations to cookbook simplicity. None of these aids is applicable to a geologic setting similar to that illustrated in figure 57I, for all of them assume an idealized geometry. The reader interested in interpreting irregular time-distance curves should consult Hawkins (1961) or Willmore and Bancroft (1960) for techniques of data processing that will lead to accurate estimates of depth.

Effect of Laterally Varying Velocities
Figure 57J

The model shown in this illustration was taken from a real example (Hawkins, 1961, fig. 6) and constitutes what might well be regarded as the general case. It is essentially a two-layer model, in which unconsolidated sediment overlies consolidated bedrock, but the boundary is irregular and the velocities in both layers vary considerably. The resulting time-distance plot is exceedingly complex. Analytical solutions of depth based on plane sloping refractors and homogeneous elastic properties would be doomed to failure under these conditions. Curves of this type are amenable to solution, however, and the hydrogeologist concerned with a geologic setting of this type is strongly advised to seek the aid of an expert in seismic refraction interpretation.

Corrections Applied to Seismic Refraction Measurements

Arrival times recorded in refraction work must be corrected to remove unwanted time variations. These variations are due to differences in elevation between individual geophones and the energy source and the presence of an irregular, near-surface layer of low velocity. The latter is referred to

commonly as the weathered layer, although this name may or may not be strictly correct geologically.

Elevation Correction

The simplest means of correcting for differences in elevation between the geophones and the shot is to convert them all to a common elevation datum by subtracting or adding the times that elastic waves would take to travel from the datum to the actual geophone or shot locations. A schematic example is shown in figure 57D. This requires knowledge of the elevation of shot and geophones and of the velocity of the medium between them and the datum. The velocity is readily obtained from refraction shooting.

Weathered-layer Correction

If an irregular low-velocity layer exists immediately beneath the surface, but is not taken into account in correcting the travel-time data, the effect will be to produce artifical variations in depth to a mapped refractor such as the buried bedrock surface. The simplest means for making this correction is to shoot it with short geophone spreads and calculate its thickness and velocity by conventional methods. This information then can be used to calculate the time delays which the weathered layer causes along those parts of the ray path near the surface, both at the shot point and at the geophones.

Errors in Seismic Refraction Measurements

A figure commonly quoted in the literature concerning the magnitude of error involved in seismic refraction depth calculations is 10 percent. Eaton and Watkins (1970) appear to substantiate this oft-quoted value with a comparison between seismically predicted depths and drilled depths at 97 drill-hole sites (fig. 58). It is notable, however, that there are 8 points in this plot which represent errors of at least 30 percent and three of these represent errors in excess of 100 percent. Such data do not reflect incompetence on the part of the geophysicists who published them, rather they represent an attempt at intellectual honesty and a willingness to reveal how far off some geophysical predictions can be. Because there is a general tendency on the part of most investigators to publish only their successful results, the data shown in figure 58 may be regarded as representing a biased sample. It is probable that the average error in most seismic refraction work is somewhat greater than 10 percent.

There are, on the other hand, published examples in which average errors in depth prediction are as small as 5 percent. The difference between these extremes of 5 and 100 percent stems, in part, from the availability of independent geologic information or other kinds of geophysical data. It should be emphasized that the more information of a stratigraphic nature the hydrogeologist can give to the seismologist, the better the seismic interpretations will be. The geophysicist, like the surveyor, benefits from being able to close on one or more control points in the form of a borehole or well. In the total absence of independent geologic or geophysical information, the interpretations can be no better than the assumptions made concerning probable conditions below the surface.

Inspection of figure 58 indicates that those depth measurements which are in error by 30 percent or more are all on the high side; the seismic method overestimated depths to the refractors. A common cause of overestimation is illustrated by figure 57H. If unrecognized velocity inversions exist in the section, an overestimate of depth is inevitable. The thickness of the slow layer and the velocity difference between it and the layer above determine the magnitude of the error.

Other sources of error pertinent to hydrogeologic studies include (1) discontinuous and abrupt lateral variations of velocity, (2) pronounced velocity anisotropy, (3) blind
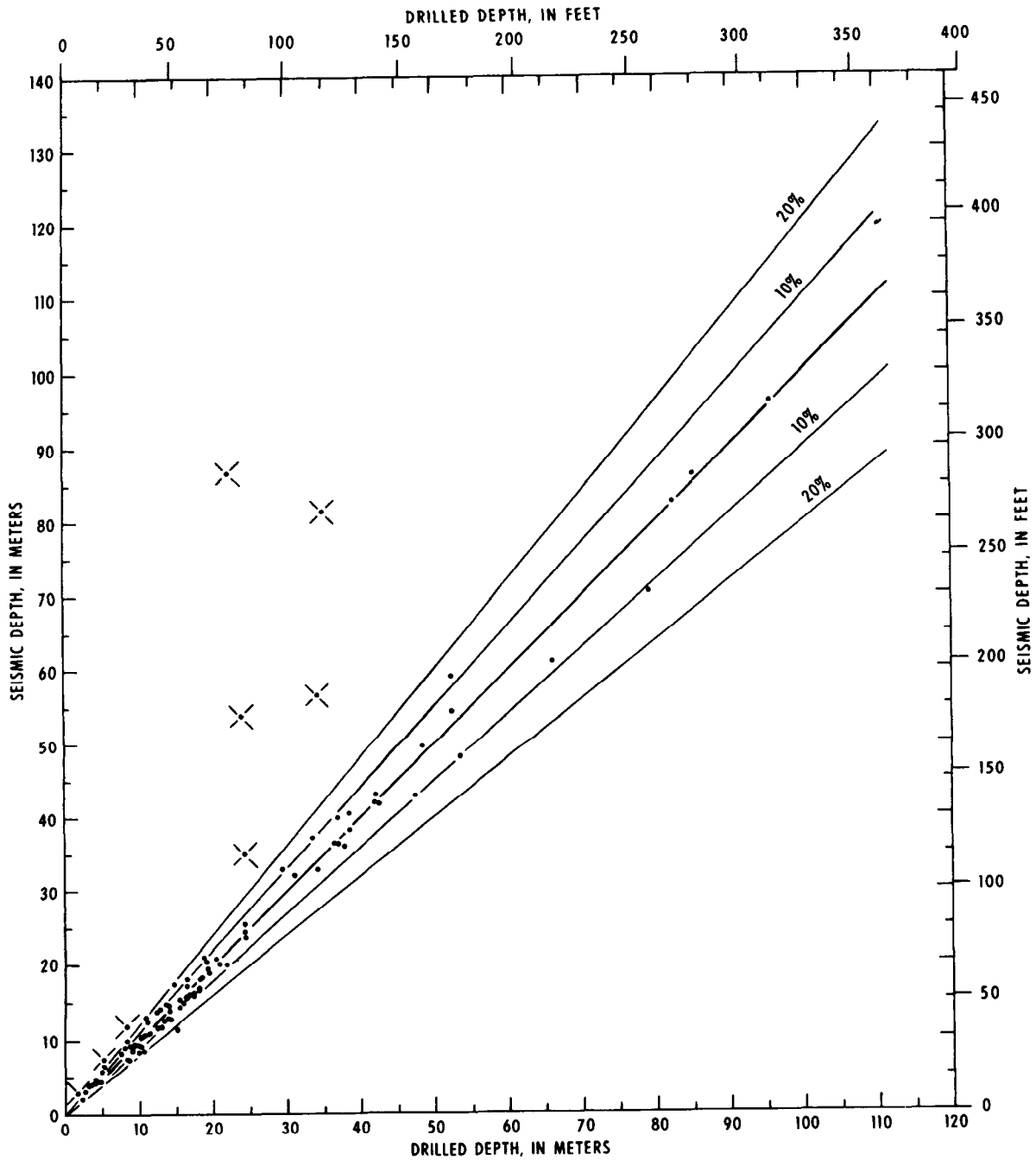
Figure 58.—Comparison of 97 seismic refraction depth determinations versus drill-hole depths at the same localities. Heavy line represents envelope of error-free determinations; labelled lines represent envelopes for errors of 10 percent and 20 percent (after Eaton and Watkins, 1970). Reproduced by permission of "Information Canada."

zones, (4) a highly fractured or weathered bedrock surface, and (5) hydrologically significant interfaces that do not display velocity contrasts large enough for seismic detection.

Applications of Seismic Refraction Measurements in Hydrogeology

Mapping Buried Channels

The most common use of the seismic method in hydrogeology is in the determination of the thickness of sediments which overlie essentially non-water-bearing consolidated bedrock. The surface of the bedrock may be plane or irregular, but it is of special hydrologic interest where it occurs in the form of a channel filled with silt, sand,

and gravel. Typical examples include the fluvial sediments of present-day river valleys and valley-train deposits in old water courses. Models of this type are particularly well adapted for seismic study if there is an appreciable contrast in velocity between the sediments and the bedrock.

A characteristic example, drawn from a study by Peterson, Yeend, Oliver, and Mattick (1968, fig. 9) is shown in figure 59. The location of this study is in northern Nevada County, California. The channel is carved in Paleozoic and Mesozoic igneous and metamorphic rocks and is filled with gravel, sand, and clay of Tertiary age. The length of the seismic refraction profile across the channel, as shown in figure 59, is 1.28 km (0.8 mile). An average geophone spacing of 30.5 meters (100 ft) was employed, and charges were fired in five shot holes ranging in depth from 1.5 to 5.0 meters (5 to 16 ft) and approximately equally spaced. All spreads were reversed.
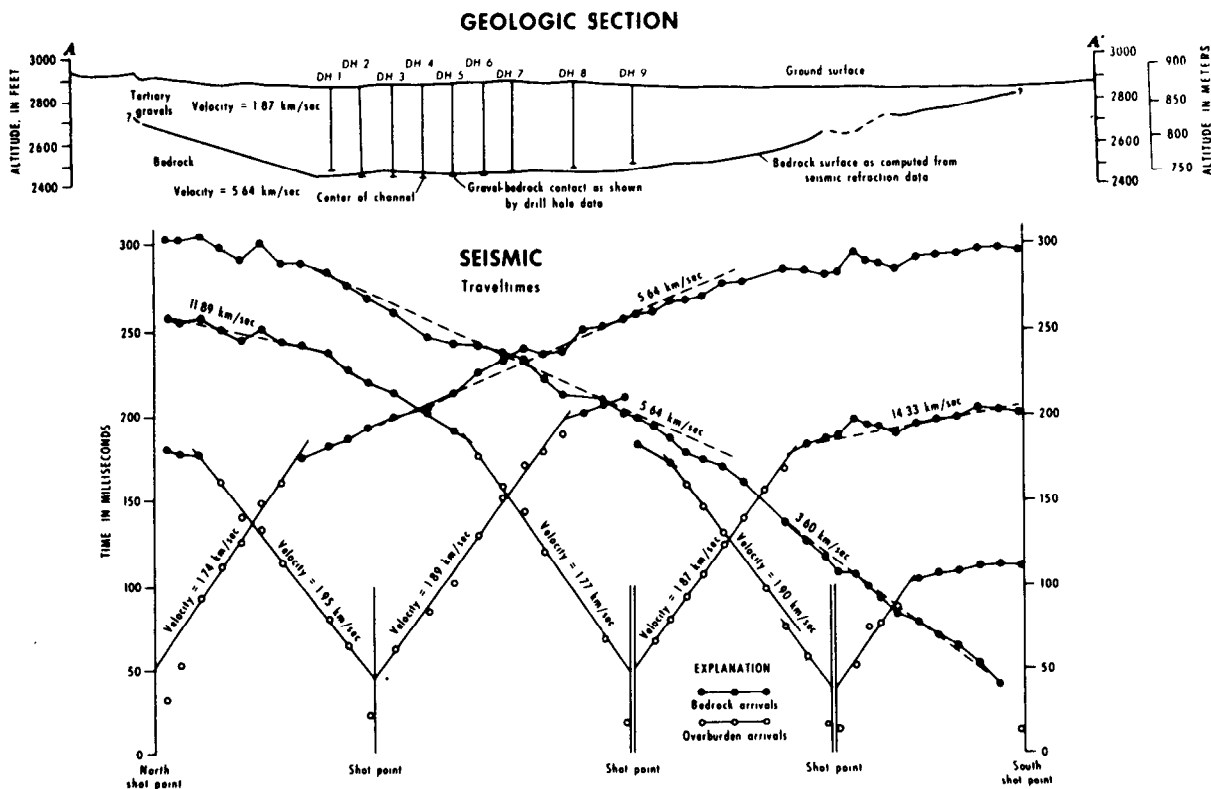

Figure 59.—Seismic cross section, drill-hole data, and traveltime curves for a buried Tertiary stream channel in northern Nevada County, California (after Peterson and others, 1968).

Dynamite charges ranged from 25 to 90 kg each. The elevations of all shot holes and geophone locations were determined to the nearest 3.0 cm (0.1 ft).

The velocity in the gravel was found from the seismic data to average 1.87 km/sec (1.16 mile/sec) and the velocity in the bedrock was 5.64 km/sec (3.51 mile/sec). On the extreme northern and southern branches of the traveltime curves, apparent velocities in excess of 11 km/sec (6.84 mile/sec) were recorded. These values are artificial and reflect the fact that the bedrock refractor is dipping toward the shot point at either end. A schematic model of a dipping refractor and its effect on the traveltime curves was shown in figure 57C.

Above the traveltime curves is a geologic cross section (fig. 59) based entirely on the seismic refraction work. Superimposed on it are vertical lines representing nine drill holes which penetrated to the buried bedrock surface. The correspondence between the two sets of bedrock depths, determined independently, is excellent. The average error in computed seismic depth for the nine holes was 4.6 percent and the maximum error, at a single hole, 8.6 percent.

A second example of a seismic refraction study of a buried valley is the work of Bonini and Hickok (1958) in northern New Jersey. This study differed from the one just described in that many more shot holes and geophone spreads were used and essentially complete areal coverage was achieved. The seismic measurements were tied closely to drill-hole control, as well.

The results of the New Jersey study are shown in figure 60, as a contour map of the buried bedrock surface. The geology of the area consists of unconsolidated glacial, alluvial, and lacustrine sediments in a buried bedrock channel carved from Triassic sedimentary rocks. Velocities in the unconsolidated sediments were found to range from 0.27 to 2.07 km/sec (0.17 to 1.29 miles/sec), and those in the bedrock, from 3.23 to 5.00 km/sec (2.00 to 3.11 miles/sec). The average error in seismic depth determinations in this study was approximately 7 percent and the
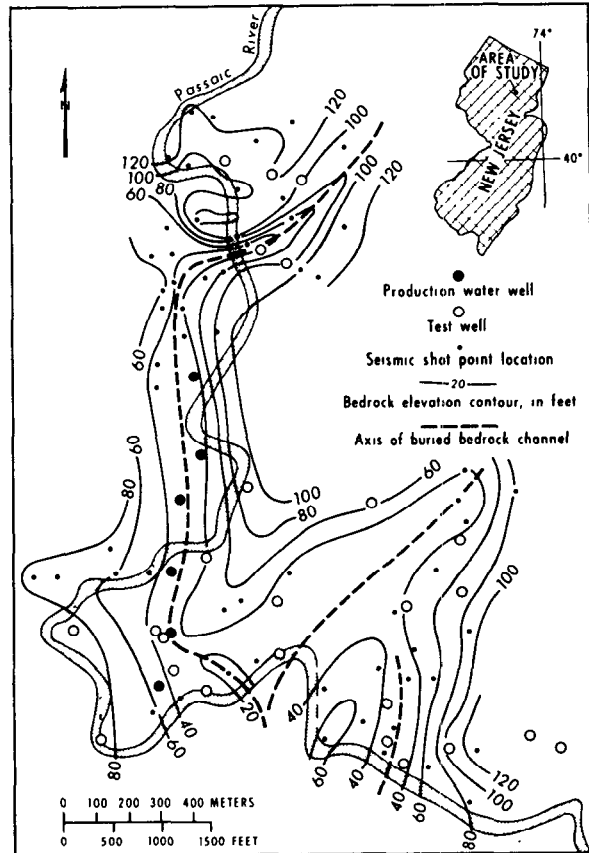

Figure 60.—Structure contours on the buried bedrock surface of the Passaic River Valley, northern New Jersey, based on seismic refraction and drill-hole measurements (after Bonini and Hickok, 1958). Reproduced with permission of Society of Mining Engineers of AIME.

maximum error, at a single hole, was 11 percent. The present-day Passaic River follows the buried bedrock channel along this reach rather closely and probably provides recharge to the aquifer.

Measuring Depths to the Water Table

Seismic refraction measurements of semiconsolidated or unconsolidated clastic deposits reveal that compressional wave velocities increase abruptly at the water table. The velocity in saturated continental sediments generally is about 1.50 km/sec (0.92 miles/sec) and is sufficiently higher than that in unsaturated sediments so that the zone of

saturation acts as a refractor. Observed velocities in unsaturated sediments generally are less than 1.00 km/sec (0.6 miles/sec), but rarely may be as high as 1.40 km/sec (0.9 miles/sec). According to Levshin (1961) the minimum observed difference in velocity across the water table occurs in fine-grained sediments and exceeds 100 to 150 meters/sec (330 to 500 ft/sec). In aquifers composed primarily of gravel he noted differences as large as 1.00 km/sec (0.62 miles/sec).

Whether or not the water table can be recognized seismically depends on the thickness of the saturated zone above the bedrock. In the discussion of figure 57G, it was noted that if the saturated zone is too thin in relation to its depth it will not appear as a separate branch on a traveltime curve prepared from first arrivals only.

Determining the Gross Stratigraphy of an Aquifer

If some of the velocity discontinuities in unconsolidated or semiconsolidated deposits represent stratigraphic breaks in the sedimentary section, seismic refraction measurements can be used, under optimum conditions to unravel the gross stratigraphy of a deposit. If these breaks further represent significant hydrologic boundaries, such as those between water-producing formations and non-water-producing formations, the seismic work may have special hydrogeologic interest. A typical example, provided by the work of Arnow and Mattick (1968), is shown in figure 61. The setting is the area between Salt Lake City, Utah, and Great Salt Lake. The study was done to determine the thickness of the valley fill so that the amount of ground water discharged toward Great Salt Lake could be estimated. The surface is underlain by Quaternary deposits of silt, sand, and clay exceeding 150 meters (500 ft) in thickness. The seismic refraction study revealed an irregular, buried bedrock surface at depths ranging from 270 meters (900 ft) to 1,460 meters (4,800 ft) below the surface. Overlying it, along part of the seismic section, is a thick section of sediments believed to be semiconsolidated sediments of Tertiary age. The velocity of these sediments is enough higher than that of the Quaternary sediments overlying them to suggest markedly different physical properties. Therefore they probably have different water-bearing properties. These older sediments would have to be taken into account in attempting to calculate the cross section of the area through which effective discharge is taking place.
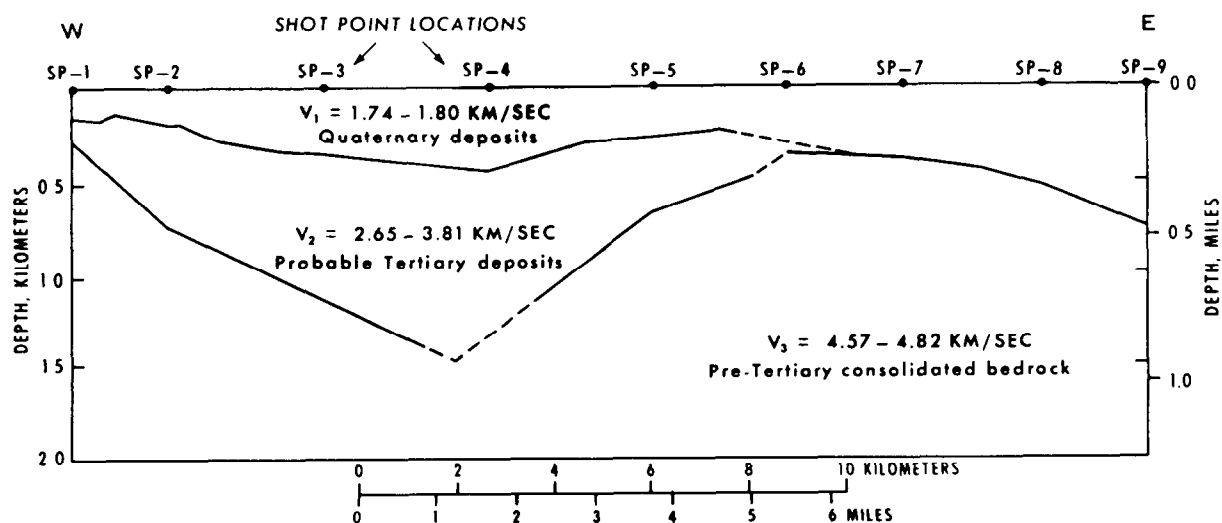

Figure 61.—Seismic cross section of the Jordan Valley east of Great Salt Lake, Utah (after Arnow and Mattick, 1968).
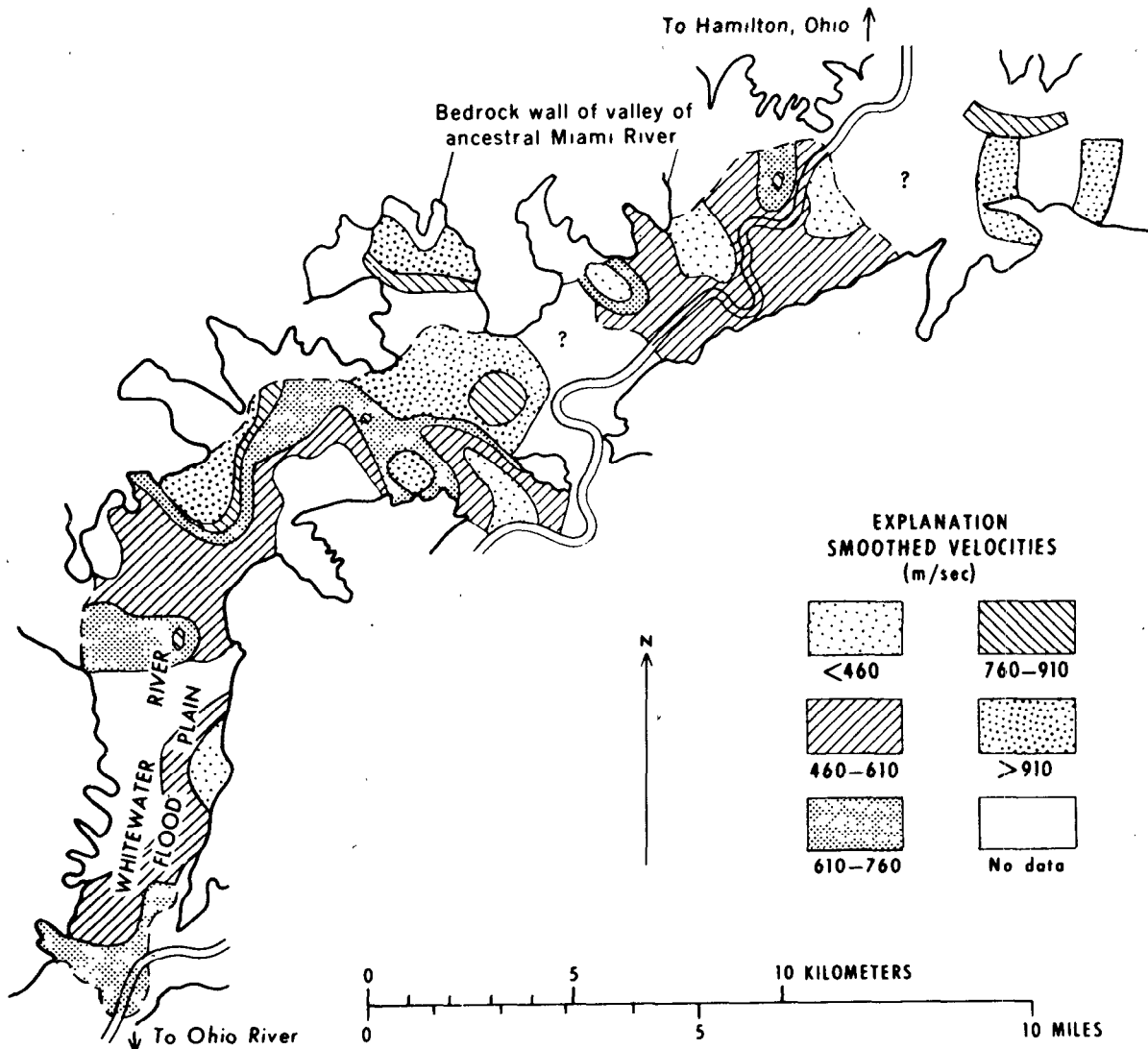
Figure 62.—Distribution of observed compressional wave velocities in unsaturated sediments of the ancestral Miami River Valley, Ohio (after Eaton and Watkins, 1970). Reproduced by permission of "Information Canada."

Another example of this kind of use of seismic refraction data is illustrated by Johnson's (1954) study of Pleistocene sediments in Illinois. Careful measurements tied to stratigraphic control at wells made it possible to distinguish drift of Wisconsin age from that of Illinoian age. In addition, water-bearing strata of sand and gravel were recognized in the section from their effect, as delayed arrivals, on the traveltime curves.

Mapping Lateral Facies Variations in an Aquifer

Seismic refraction measurements in areas where a large number of geophone spreads and shot points are employed, may reveal systematic lateral variations in the velocity of unconsolidated deposits. These variations reflect measurable variations in the physical properties of the deposits, which in turn stem from fundamental variations in lithology. Many geologic factors contribute to variations in the compressional wave velocity of unconsolidated and semiconsolidated sediments. Among these are geologic age, average grain size, grain-size distribution, composition, degree and nature of cementation, confining pressure, degree of saturation, and porosity.

A paper by Eaton and Watkins (1970)

shows the distribution of compressional wave velocities in unsaturated outwash sand and gravel in the valley of the ancestral Miami River in southwestern Ohio (fig. 62). The velocity variations represent lithofacies variations in the upper 30 to 100 meters (100 to 300 ft) of the valley fill. A correlation of water wells of high productivity with areas of a given velocity value would allow use of the seismic velocity map for locating additional well sites of potential high productivity.

Estimating Porosity from Seismic Wave-Velocity Values

Many investigators have noted a pronounced correlation between porosity and compressional wave velocity in clastic sediments, velocity increasing with decreasing porosity (fig. 63). Similarly, there is a correlation between velocity and density, velocity increasing with increasing density. These correlations of porosity and density with seismic wave velocity are interdependent, as bulk density can be defined by three parameters:

porosity, grain density, and pore-fluid density. For a group of sediments with the same average mineralogical composition and saturated with ground water of approximately uniform composition, variations in bulk density are a function primarily of variations in porosity. If a small amount of cementing material is present in the pores, it would diminish total porosity but at the same time increase bulk density. Assuming the composition, and more particularly the grain density, of the cement to be approximately the same as that of the clastic constituents, its presence would not materially affect the relationship between density and porosity. In such a situation, the cement could be regarded macroscopically as one of the mineral constituents of the sediment. If its composition is grossly different from that of the clastic grains, however, variations in the degree of cementation would result in variations in the average grain density of the sediment, and the simple relationship between porosity and bulk density would not hold. Neither would that between porosity and velocity. Other factors, such as the degree of
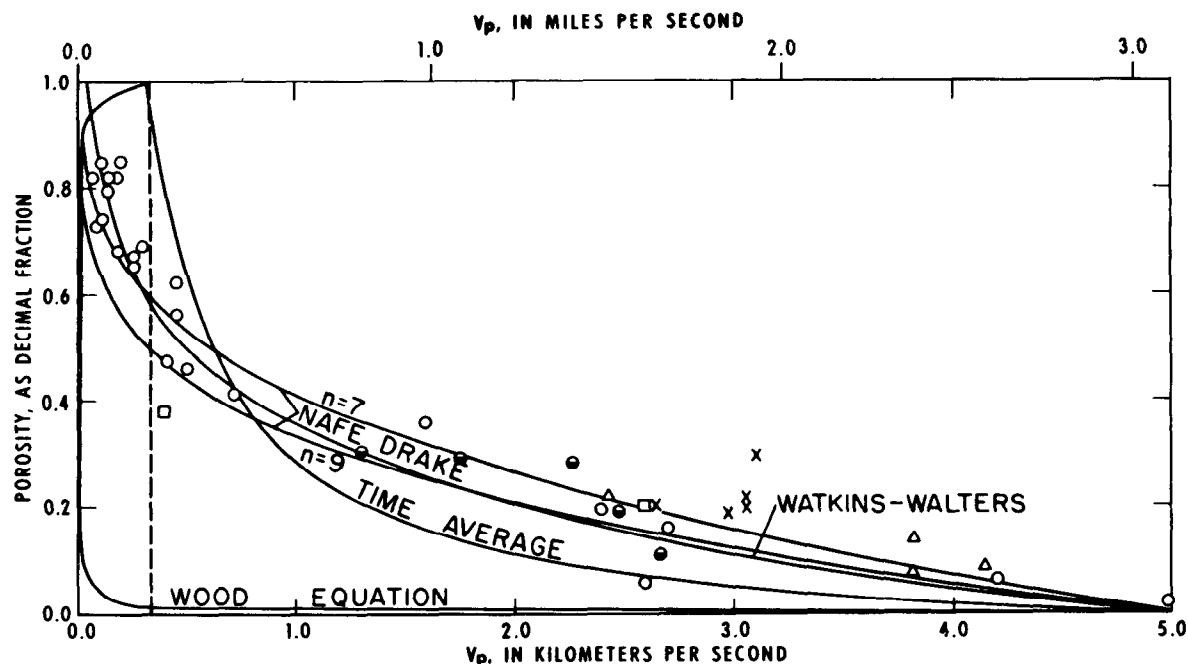

Figure 63.—Plot of observed porosity versus compressional wave velocity for unconsolidated sediments (after Eaton and Watkins, 1970). Reproduced by permission of "Information Canada."

fracturing in a semiconsolidated rock, also influence velocity, the greater the volume density of fractures, the lower the velocity. To some extent, however, fractures contribute to the total porosity, so their effect on the velocity-porosity relationship is not always pronounced. The net result is that velocity values can be used to predict total average porosity, within certain limits, for unconsolidated sediments and weakly consolidated sedimentary rocks.

Experimental data bearing on the systematic relationship between velocity and porosity (fig. 63) include rocks and sediments of a wide variety of compositions. The smooth curves drawn through the data points are empirically derived mathematical functions relating the two properties. Curves such as these could be used in conjunction with mapped velocities like those in figure 62 to produce maps illustrating areal variations in porosity for uniform sediments in a given area. Although the standard deviation of porosity determined in this way would be high, the maps might nevertheless serve a useful purpose in evaluating the relative water-storage potential of the sediments.

References Cited

Arnow, Ted, and Mattick, R. E., 1968, Thickness of valley fill in the Jordan Valley east of the Great Salt Lake, Utah, in Geological Survey Research 1968: U.S. Geol. Survey Prof. Paper 600-B, p. B79-B82.

Bonini, W. E., and Hickok, E. A., 1958, Seismic refraction method in ground-water exploration: Am. Inst. Mining Metall. Engineers Trans., v. 211, p. 485-488.

Dobrin, M. B., 1960, Introduction to geophysical prospecting: 2d ed. New York, N. Y., McGraw-Hill Book, Co., Inc., 446 p.

Eaton, G. P., and Watkins, J. S., 1970, The use of seismic refraction and gravity methods in hydrogeological investigations, p. 544-568 in Morley, L. W., ed., Mining and Groundwater Geophysics, 1967: Geol. Survey Canada, Economic Geol. Rept. 26, 722 p.

Hawkins, L. V., 1961, The reciprocal method of routine shallow seismic refraction investigations: Geophysics, v. 26, p. 806-819.

Johnson, R. B., 1954, Use of the refraction seismic method for differentiating Pleistocene deposits in the Arcola and Tuscola quadrangles, Illinois: Illinois State Geol. Survey Rept. Inv. 176, 59 p.

Kaufmann, H., 1953, Velocity functions in seismic prospecting: Geophysics, v. 18, p. 289-297.

Levshin, A. L., 1961, Determination of ground-water level by the seismic method: Akad. Nauk. SSSR IZU. Ses. Geofiz, no. 9, p. 857-870.

Peterson, D. W., Yeend, W. E., Oliver, H. W., and Mattick, R. E., 1968, Tertiary gold-bearing channel gravel in northern Nevada County, California: U.S. Geol. Survey Circ. 566, 22 p.

Slotnick, M. M., 1959, Lessons in seismic computing: Soc. Exploration Geophysicists, Tulsa, 268 p.

Soske, J. L., 1959, The blind zone problem in engineering geophysics: Geophysics, v. 24, p. 359-365.

Willmore, P. L., and Bancroft, A. M., 1960, The time term approach to refraction seismology: Royal Astron. Soc. Geophys. Jour. (London), v. 3, p. 419-432.